

# Image Quality Assessment in the Context of the Brazilian Electoral System

Marcondes Ricarte da Silva Júnior<sup>1</sup><sup>a</sup>, Jairton da Silva Falcão Filho<sup>1</sup><sup>b</sup>, Zilde Souto Maior Neto<sup>1</sup><sup>c</sup>,  
Julia Dias Tavares de Souza<sup>1</sup> Vinícius Lima Ventura<sup>1</sup> and João Marcelo Teixeira<sup>2</sup><sup>d</sup>

<sup>1</sup>Informatics Center, Universidade Federal de Pernambuco, Recife, Brazil

<sup>2</sup>Electronics and Systems Department, Universidade Federal de Pernambuco, Recife, Brazil

Keywords: LCD Screen, OCR, Blur, No-reference, Image Quality.

Abstract: The Brazilian electoral system uses an electronic voting machine to increase the voting reliability. This voting machine goes through a series of security procedures, and the one that uses the most human resources is the integrity test. The proposed solution to optimize these resources is using a robotic arm and computer vision methods to replace the eight persons needed to carry out the test currently. However, there is a problem with the LCD screen in the poll worker's terminal. There is no backlight on the LCD screen, this may cause visual pollution on images captured by the camera, depending on the ambient lighting and camera position. In this way, this paper proposes two methods to make it easier to choose the best images to be used in the extraction of information process: OCR and blur analysis. We analyzed 27 images with three ambient lighting configurations then compared our results with three no-reference image quality evaluators and research on human perception of image quality. The OCR analysis matched very closely the human perception and the other evaluators.

## 1 INTRODUCTION

The Electoral Justice is the Brazilian governmental agency responsible for the entire electoral process for the whole country, including all states and cities elections. The Supreme Electoral Court (TSE) is the highest organ on a federal level, and the headquarters are based in the Brazilian capital, Brasilia. As for the states/provinces, the Regional Electoral Courts (TREs) are the ones responsible for the elections. These agencies together are the authority for all steps in the electoral process, from the electoral register to the diplomacy of the elected, passing through the voting stage (Court, 2020).

The Brazilian electoral process started to change in 1995 when the TSE started the genuinely Brazilian electronic voting machine project. This project replaced the slow and susceptible fraud process of manual counting in paper ballot elections that came with errors and widespread suspicion. Then in 1996,

in municipal elections, 57 cities had the first contact with the electronic voting machine, counting the vote of more than 32 million Brazilians. Furthermore, in the 2000 elections, Brazil started the first fully computerized election (Court, 2022c).

The electronic voting machine is a microcomputer explicitly used in elections and is composed of two terminals: the poll worker's terminal and the voter terminal. The first consists of a numeric keyboard, a Liquid Crystal Display (LCD), and, in some models, a biometric reader. In this first one, the voters' identification and authorization to vote are carried out. The second has a numeric keyboard and a Light Emitter Diode (LED) screen, where the vote is privately registered (Court, 2022b).

Security tests are performed on the electronic voting machine every election year. Its primary process is known as the "Electronic Voting Machine Integrity Test" ("Teste de Integridade das Urnas Eletrônicas" in Portuguese) and aims to demonstrate the functioning and security of the electronic voting machine. This process begins the day before the election; a series of local polling stations are randomly selected to have their electronic voting machine tested. The number selected from each state is proportional to the total

<sup>a</sup> <https://orcid.org/0000-0003-0359-6113>

<sup>b</sup> <https://orcid.org/0000-0001-6383-7551>

<sup>c</sup> <https://orcid.org/0000-0001-5993-2062>

<sup>d</sup> <https://orcid.org/0000-0001-7180-512X>

number of polling stations used for that voting round.

Regarding the votes that will be cast at the integrity test, the TREs provide several ballots that correspond between 75% and 82% of that polling station voters. That is because to realize a proper test is necessary to account for the absentees, therefore it is not necessary to have 100% of voters. As for the candidates chosen, the parties are invited to fill the ballots used in the audit before the election week. Also, school kids that cannot vote yet are chosen to fill ballots to complete the total number of votes necessary in the electronic voting machine. Then, on election day, simultaneously with the actual election, the audit begins with the verification that there are no votes inside the equipment. Then, all votes obtained with the filled ballots are entered one by one in the electronic voting machine and into a computer at the same rate as an auxiliary system for confirmation. At the end of the voting process, the electronic voting machine prints a Ballot Report (BU), and the auxiliary system also issues a report. Finally, all the data are compared, verifying if the electronic voting machine had its normal functioning as expected (Fachin, 2021).

Approximately eight people per electronic voting machine are involved in this process, divided in two rounds. The first person takes the paper ballot that was filled out and checks its validity, the second enters a valid title with the votes on the ballot in the auxiliary system, the third qualifies the voter in the poll worker's terminal and the fourth enters each digit of the vote in the voter's terminal (Court, 2022a).

To minimize human interference increasing security and confidence of the integrity test, we are developing an alternative that uses a robotic arm aided by computer vision. In the test, the robot performs the functions of typing the voter's title in the poll worker's terminal and the votes in the voter's terminal, removing human interference in these actions, only one person is needed to change the ballot. The solution using the robotic arm to automate the integrity test received an innovation award.

A camera attached to the robotic arm is used to extract, from each ballot, the title and the votes to be typed by the robot and subsequently to view the screen and validate what was typed at the terminals and ensure that the information extracted from the ballots is the same as typed on the screen, ensuring the integrity test.

The technique used to extract the information will be Optical Character Recognition (OCR). According to Tekin (Tekin et al., 2011), LCD screens have some characteristics that make them difficult to read by OCR, such as low contrast and proximity of the edge of the numbers to the edge of the screen. In addition,

depending on the camera's position, there may be reflections or shadows on the screen that superimposes the information.

The main objective of this work is to present metrics to classify images on the screen of the poll worker's terminal regarding their quality for extracting information and thus defining the best position of camera for extraction of information on the screen and thus ensure a more reliable automation system because the electronic voting machines are distributed throughout Brazil and with that there are several lighting scenarios. And doing so we intend to validate the classification of the same images by people and three no-reference image quality scores: BRISQUE (Mittal et al., 2012a), PIQE (Chan and Goldsmith, 2000), and NIQE (Mittal et al., 2012b).

The remainder of this paper is structured as follows. Section 2 list some works related to the proposed solution. Section 3 describes the methodology used to classify the images. Section 4 presents the results obtained with the analyses and metrics used. Finally, on section 5 we expose the conclusions of this paper.

## 2 RELATED WORKS

In this section, we present works that discuss image quality analyzer with reference and no-reference methodology and OCR on screen.

### 2.1 Image Quality Analyzer

Image quality analysis is usually performed on databases with prior human evaluation. Qin and El-Yacoubi (Qin and El-Yacoubi, 2017) presents a Deep Neural Network (DNN) trained to predict the quality of finger vein images is proposed. Some approaches applied to two public datasets were compared, where the best results were for Patch-DNN. Mittal, Soundararajan, and Bovik (Mittal et al., 2012b) deal with a blind image quality analysis that uses measurable deviations from statistical regularities for natural images without training on human opinions. The proposed index scored better than the Popular Signal-to-Noise Ratio (PSNR) and Structural Similarity Index (SSIM) and is equivalent to high-performance image quality analysis approaches. Courtney (Courtney, 2021) analysis the image quality of non-referenced documents to select the best image for the OCR application automatically. It used a metric based on character feedback and checked the parameters influencing OCR extraction, e.g., noise, blur, contrast, and brightness, seen as the most signif-

icant influencers. The OCR solution used was Tesseract (Smith, 2007). The metric validation was done with images created with influence on the parameters mentioned compared with other indexes: BRISQUE, NIQE, and PIQE. Furthermore, in comparison, the suggested index could define the best image for OCR extraction in all dataset images.

## 2.2 OCR

Optical character recognition is a computer vision technique for extracting characters from images and documents. Kastelan et al. (Kastelan et al., 2012) use a system for OCR text extraction on the TV screen to validate the operation of the TV by comparing the extracted information with the expected text using Tesseract. Vellian et al. (Mariappan et al., 2011) proposes a system for extracting characters from LED and LCD screens in real-time, passing the information through sound, is discussed to assist people with visual impairments. They use adaptive binarization and an approach to extract “blobs,” which serves to identify the highest probability of identifying possible digits. In tests, average error rates of 1.19% and maximum error rates of 1.52% were obtained. Tekin et al. (Tekin et al., 2011) also use OCR for character extraction of an LCD screen, but for multiple medical instruments. The system works with three simultaneous screens, and the technology used is the LabView Vision Assistant OCR (Kwon and Ready, 2014). The OCR is trained with images from the LCD screen repeatedly until it can extract the characters accurately. In the end, the system presented a 100% success rate for the ten tests performed.

## 3 METHODOLOGY

In this section we describe all the steps used to obtain the scores. We create the dataset of the terminal screen images with the assistance of a robotic arm. We analyzed the OCR character extraction and blur for all images. To validate the result we compared with three image quality evaluators no-reference and verified the result with people’s perception with the application of surveys.

### 3.1 Dataset

First, to perform the blind analysis, it was necessary to create a dataset composed of different images that brought to the experiment a diversity of positions and contrasts to simulate a layman user operating the system. Therefore, initially 9 fixed positions were se-

lected for the camera focusing on the terminal screen, being three positions with height variation: above the screen (P1), over its center (P2) and below it (P3), in which each one had two auxiliary positions: to the left (P-L) and to the right (P-R). These positions are exemplified in Fig.1.

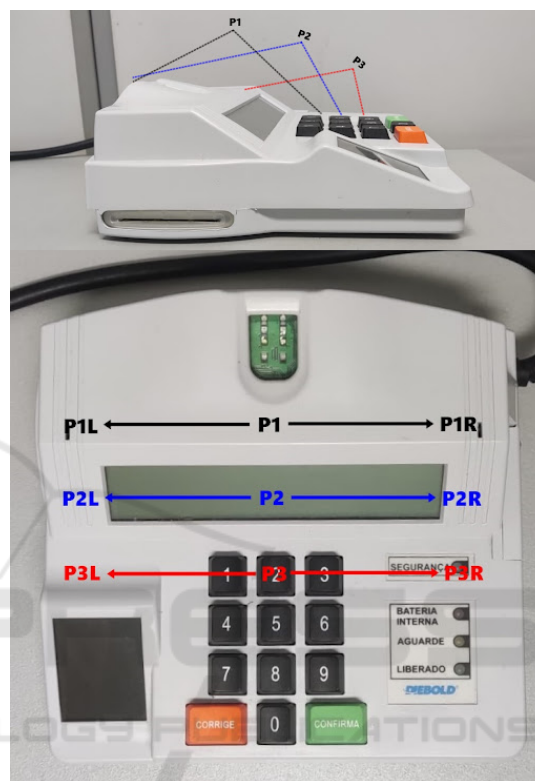


Figure 1: Illustration of positions for the camera for the terminal screen. First the side view demonstrating the height variation of the central positions, and then all positions in the top view.

In addition to the position variation, a lighting variation was also made in a room with little natural light irradiation. However, the place has 24 LED tubes with 18 W of power, divided into 12 luminaries. These are arranged in four rows with three luminaries each. Three types of lighting were used: no lighting, partially lit and fully on. The first configuration has all lights off, the second with half of the lights on, and the last with all lights on. To ensure that in each lighting variation we would have the same relative position, we had the help of a COMAU eDO (COMAU, 2021) robotic arm. A Logitech C922 HD webcam was attached to the robotic arm being taken to the 9 defined positions, in the three different illuminations conditions following the same order. Thus, 27 images were obtained to be analyzed. It is important to note that the information on the screen does not vary. Subsequently, a correction was made in the images with

focus only on the poll worker's terminal screen, isolating the screen. The four points used for perspective distortion correction were selected manually and used a function from the OpenCV (Bradski, 2000) library for perspective change. With the dataset finalized, the image analysis phase began. The dataset images can be seen in Fig.2.

In the link there is a video showing the robotic arm passing through the positions used to obtain the images of the poll worker's terminal screen.



Figure 2: Dataset of images of the terminal screen.

### 3.2 OCR Analysis

The terminal screen has 4 lines with 40 cells per line. For the criterion of OCR extraction each image was cut into 160 rectangular cells, to separate the screen image into every possible character space. Python code was used to automate this process. Fig.3 shows the demarcation of each cell obtained for an image of the data.



Figure 3: Image of terminal screen with the cutout markings.

The clipping is done by ranging each line separately. The default width for the number of cells per line should be equal to 30 pixels due to the image width being equal to 1200 pixels, but to try to minimize the errors caused by the distortion caused by the perspective change, 2 pixels on each side were added, totaling 34 pixels, which can be seen in the lateral overlay of the rectangles with different colors, in Fig. 3. There are two exceptions caused by the side edges of the image, which makes the first cell of

each row 30 pixels wide and the last 32 pixels wide. The default height for the number of cells per column should be equal to 74 pixels, since the height of the image is 296 pixels, however, for the same reason of the width variation, it increased 3 pixels on each side, totaling 80 pixels, this value was used for lines 2 and 3. For the first line the height used was 74 pixels and for the last line 71 pixels.

The images are then pre-processed before applying the OCR. In this step, only color space transformation was used, from RGB to grayscale, and then an adaptive thresholding from the OpenCV library was applied, with blockSize equal to 11 and the value of the constant that is subtracted from the average equal to 3. This binarization technique segments the image based on a threshold that dynamically changes over pixel regions of the image. This sequence was used to try to make the character clearer for the OCR and as this is a blind analysis, the objective is not to analyze if the OCR correctly returned the characters, but to verify if it can identify that there are any characters. Fig.4 shows some characters from the original image and after pre-processing.

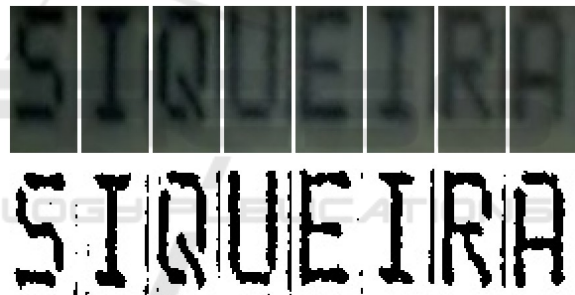


Figure 4: Example with 8 cells before and after pre-processing.

With the binarized images, EasyOCR (Awalgaonkar et al., 2021) was used to recognize the characters. This OCR was used because it needs less pre-processing, extracting the text from the images more directly.

After having the result of the set of cells per image, an initial pattern is created as an initial reference of the image information, being verified which character is most repeated, thus finding the mode between a given cells in the 27 images. When there is one more of eligible character as mode per cell, that cell in the initial reference becomes empty. Next, a comparison is made between the initial reference and the character is extracted per image and thus a value is assigned to each image, termed the initial score. This value is the number of characters that belong to the image and the initial reference, divided by the number of characters contained in the initial reference, disregarding spaces.

Fig.5 exemplifies how the initial result was obtained.

Based on the final score the final reference is built. The empty spaces that were left in the initial reference for having more than one mode per position are filled with the characters in which the image has the highest initial score. Afterwards, another comparison is made between the images and the final reference, following the same methodology of the initial score, to define the final score per image. In Fig.6 the logic that was used is exemplified.

### 3.3 Blur

The blur level defines how difficult the objects in the scene could be seen, eventually related to bad camera focus. It is an important metric for evaluation because it causes some problems for edge detection techniques due to the absence of edges in blurred images. With this in mind, our focus on this metric aims to define the blur level of an image, quantifying how blurred is an image.

Pech-Pacheco et al. (Pech-Pacheco et al., 2000) and Bansal et al. (Bansal et al., 2016) show a proposal for the use of the *Laplacian Operator* to obtain a metric to evaluate blur in an image. As this operator is often used for edge detection (Shrivakshan and Chandrasekar, 2012), the variance of the responses from detected edges can provide a metric to classify an image as blurred or not.

This variance defines the edge responses of the image which the operator has applied. So, as high it is means that there are a lot of edge responses indicating that many edges are detected, and as low it is represents detection of very little edges on the image. The problem with the variance is that it is very domain-dependent, so after analyzing how this variance performs on our dataset we decided to clamp the values to the range [3, 30] where as low the value most blurred is the image.

### 3.4 Metrics Comparison

In order to validate our approach we applied our dataset to 4 metrics: survey, BRISQUE, PIQE, and NIQE.

For the survey metric have been applied three surveys where each have nine images of a single light variation has been explained in Dataset subsection. The first with images 1-9, regarding a poorly lit room, got 10 answers. The second covered the pictures 10-18, regarding a partially lit room, had 11 answers. And the third survey was answered by 20 people with the images 19-27 taken in the fully lit room.

This metric function is to determine what a regular person perceived as a good image in a quantified way. For that reason all three surveys had the same ten standardized questions where which answer could provide the image with point. These points will be add up and then divided by the number of people on that survey, therefor making the image official score.

Initially everyone was asked to rank their top 3 images in that specific poll, the first position earn the image 3 points, the second two and the third one point. Then, so all images could be analyzed and we could get a better take on what a person looks for a good image we asked them to describe the images in one of this six sentences:

- I am not able to read any character (no points);
- I am able to read some characters (2 points);
- I am able to read most of the characters and understand some words (3 points);
- I am able to read most of the characters and understand all of the words even though they are incomplete (4 points);
- I am able to read all the characters and all words (5 points);

Therefor all images could get up to eight points if it got chosen as best picture and people were able to read every character in the screen.

BRISQUE, PIQE, and NIQE were used because they are no-reference image quality score. The first is Blind/Referenceless Image Spatial Quality Evaluator. Second is Perception based Image Quality Evaluator. And the last is Naturalness Image Quality Evaluator. To obtain the value of these metrics the algorithms of (Aggarwal, 2020) were used. Your scores are in the range 0 to 100. For all, evaluators a smaller score indicates better quality.

## 4 RESULTS

Here we present the results for the presented metrics. First, we ran each metric separately on the dataset, obtaining the scores for each image. After, we discuss about the presented results, explaining how well each one has behaved and discussing about them, finishing showing our performance by making the comparison between it and the results from the survey and some techniques in the literature.

### 4.1 OCR

The final score of each image was put into Table 1, it can be seen that the image that scored the best is

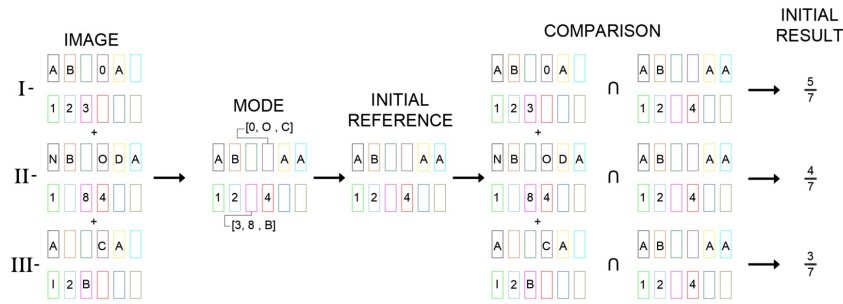


Figure 5: Illustration the creation of the initial result.

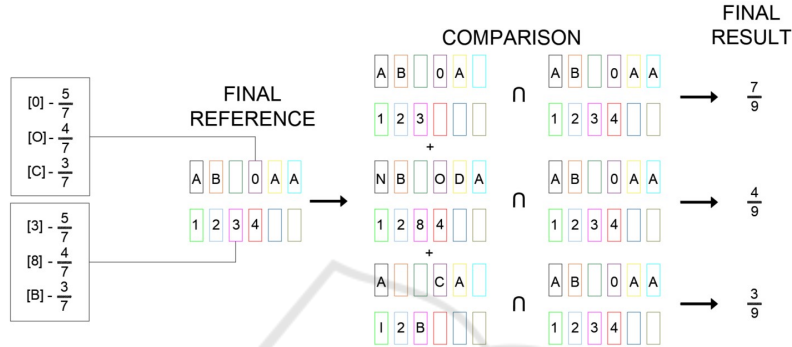


Figure 6: Illustration the creation of the final result.

image 24, which belongs to the subgroup of full illumination and P2L position. Analyzing by subgroup, no illumination had the worst result, with 7 images scoring 0 and an average of 0.34 points. The best subgroup was the one with total illumination, which has the image with the best score and an average of 12.50 points, while partial illumination has an average of 5.90 points.

By position, P2L obtained the highest average, with 15.10 points, and P1R had the worst average, with 0.52 points. Among them and in descending order of average, there are: P3L with 9.90 points, P3 with 8.85 points, P1L with 5.72 points, P2 with 4.69 points, P1 and P3R both with 4.17 points and P2R with 3.13 points.

## 4.2 Blur

As discussed in the previous section, the Blur metric provides us a variance value that depends on the domain, where after some tests we have decided to clamp the values in the range [3,30]. Looking forward, as our goal is to apply these values in the proposed formula we have made a simple linear conversion obtaining values in the range [0,1]. Tab. 1 contains the results for the blur metric for each image. Note that the higher is the value, the sharper is the image, so it has better quality.

As we can see, the generated results are quite rea-

sonable: for the images 1 to 9 that represents the image with no luminosity we have really low values, mainly due to the absence of edges because no features can be really detected on the image. For the images 10 to 18 as we have more edges recognized in the image due to the luminosity the results increased a lot, and for the images 19 to 27 as we have the total luminosity the characters are most sharpness.

## 4.3 Comparative with Metrics and Survey

The results obtained with the surveys are contained in Tab. 1. Based on human perception, the image with the best quality is 26 and the worst are 1, 2 and 3.

Table 1 contains the result for all images for OCR analysis, blur analysis, the metrics no-reference, the survey and voter's title extraction, all in percent. For OCR, blur and survey highest score indicates better perceptual quality but for BRISQUE, PIQE and NIQE, a smaller score is better. The best scores per column and the number of the respective images are in bold.

With Table 1 it can be seen that our OCR analysis and the BRISQUE metric elected image 24 as the best image. For our blur analysis two images are elected the best, 19 and 23. For PIQE the best image is 2 and for NIQE the best image is 8. According the survey the best image is 26. For the worst images there was

Table 1: Results of OCR, BLUR, BRISQUE, PIQE, NIQE and survey.

N°	OCR	BLUR	BRISQUE	PIQE	NIQE	SURVEY
1	1.56	6.92	55.66	71.53	16.09	0.00
<b>2</b>	0.00	1.77	64.5	<b>14.29</b>	12.98	0.00
3	0.00	1.82	60.68	41.4	14.36	0.00
4	0.00	1.9	64.27	80.69	14.78	17.50
5	0.00	2.66	62.06	20	16.85	37.50
6	0.00	5.18	56.85	69.03	14.5	41.25
7	0.00	5.94	57.15	68.06	14.27	36.25
<b>8</b>	0.00	4.28	58.79	43.78	<b>11.91</b>	13.75
9	1.56	2.26	61.96	32.91	12.57	10.00
10	3.12	48.61	55.79	60.15	17.89	45.50
11	1.56	16.49	63.83	69.14	15.58	19.25
12	0.00	20.59	60.6	69.52	15.33	14.75
13	4.69	33.94	59.67	49.13	13.16	71.63
14	4.69	54.78	60.17	56.02	12.69	47.75
15	12.50	40.46	58.31	52.82	13.28	71.63
16	10.94	22.53	59.46	49.08	13.19	54.50
17	14.06	9.8	59.98	44.9	13.47	77.25
18	1.56	15.34	59.59	52.93	14.12	60.25
<b>19</b>	12.50	<b>100</b>	52.59	42.33	14.36	10.63
20	10.94	29.05	61.01	54.5	14.39	2.50
21	1.56	62.81	64.97	53.08	14.07	14.38
22	4.69	59.52	58.23	48.98	15.18	65.00
<b>23</b>	9.38	<b>100</b>	55.1	45.84	13.69	43.13
<b>24</b>	<b>32.81</b>	86.43	<b>46.26</b>	41.71	13.59	49.38
25	18.75	46.81	60.74	56.56	14.16	52.50
<b>26</b>	12.50	40.3	63.92	69.13	13.29	<b>79.38</b>
27	9.38	47.68	62.84	62.86	14.03	70.63

Table 2: Values of Spearman correlation coefficient.

	SURVEY	BRISQUE	PIQE	NIQE
OCR	0.574	-0.246	-0.094	-0.266
BLUR	0.422	-0.365	0.063	-0.018

no similar result, our OCR analysis elected image 6, our blur analysis elected image 2, for BRISQUE is 21, for PIQE is 4, for NIQE is 10 and for survey three images obtain zero score: 1, 2 and 3.

The best image for OCR analysis was ranked only 9th in human perception. The best images for blur analysis were ranked 22 and 12. Images 2 and 3 were considered the worst in the survey and in the OCR analysis, and image 2 was also considered the worst for blur analysis.

To verify the correlation between the metrics, Spearman's correlation was used. The values of the coefficients are contained in Table 2. It can be seen that the OCR rating has a moderate correlation with the survey while the Blur rating has a weak correlation. PIQE has an almost zero correlation with both approaches while BRISQUE and NIQE have a negative and weak correlation.

## 5 CONCLUSION

The work presented in this paper describes two methods used to analyze the quality of the clerk's terminal screen image by comparing the results with three no-reference image quality score and a survey.

It was seen that for the best quality analysis for LCD screen extraction the OCR analysis obtained the best result compared to human perception and other metrics in the literature, which is validated by having the best correlation with human evaluation. Its use is recommended to choose the best image to extract information from the screen of the poll worker's terminal.

Proposition for future work would be the use of the proposed evaluator as an OCR analysis to define the best position for the robot used in the automation of the electronic voting machine integrity test with more evaluation positions and screen extraction automation.

## ACKNOWLEDGEMENTS

This work has been supported by the research cooperation project between Softex (with funding from the Ministry of Science, Technology and Innovation—Law 8.248) and CIn-UFPE.

## REFERENCES

- Aggarwal, A. (2020). Buyizhiyou/nrvqa: No reference image/video quality assessment (brisque/niqe/piqe/diqa/deepbiq/vsfa). url= <https://github.com/buyizhiyou/NRVQA>. Accessed: 2022-09-15.
- Awalgaonkar, N., Bartakke, P., and Chaugule, R. (2021). Automatic license plate recognition system using ssd. In *2021 International Symposium of Asian Control Association on Intelligent Robotics and Industrial Automation (IRIA)*, pages 394–399. IEEE.
- Bansal, R., Raj, G., and Choudhury, T. (2016). Blur image detection using laplacian operator and open-cv. In *2016 International Conference System Modeling & Advancement in Research Trends (SMART)*, pages 63–67. IEEE.
- Bradski, G. (2000). The opencv library. In *Dr. Dobb's Journal: Software Tools for the Professional Programmer*, volume 25, pages 120–123. Miller Freeman Inc.
- Chan, R. W. and Goldsmith, P. B. (2000). A psychovisually-based image quality evaluator for jpeg images. In *Smc 2000 conference proceedings. 2000 ieee international conference on systems, man and cybernetics: cybernetics evolving to systems, humans, organizations, and their complex interactions'(cat. no. 0, volume 2, pages 1541–1546. IEEE.*
- COMAU (2021). e.do robot. url= <https://edo.cloud/en/learning-center/>. Accessed: 2022-07-20.
- Court, R. E. C. (2022a). Como ocorre o teste de integridade das urnas eletrônicas. url= <https://www.trece.jus.br/eleicao/eleicoes-2022/auditoria-de-funcionamento-das-urnas-eletronicas/como-ocorre-a-auditoria-de-funcionamento-das-urnas-eletronicas>. Accessed: 2022-11-16.
- Court, S. E. (2020). Processo eleitoral no brasil. url= <http://www.tse.jus.br/eleicoes/processo-eleitoral-brasileiro>. Accessed: 2022-10-10.
- Court, S. E. (2022b). Ballot box. url= <https://international.tse.jus.br/en/electronic-ballot-box/presentation>. Accessed: 2022-07-22.
- Court, S. E. (2022c). Urna eletrônica 25 anos: Lançado em 1996, equipamento É o protagonista da maior eleição informatizada do mundo. url= <https://www.tse.jus.br/comunicacao/noticias/2021/Maio/urna-eletronica-25-anos-lancado-em-1996-equipamento-e-o-protagonista-da-maior-eleicao-informatizada-do-mundo>. Accessed: 2022-08-12.
- Courtney, J. (2021). Sediqa: Sound emitting document image quality assessment in a reading aid for the visually impaired. In *Journal of Imaging*, volume 7, page 168. MDPI.
- Fachin, E. (2021). Resolução nº 23.673, de 14 de dezembro de 2021. url= <https://www.tse.jus.br/legislacao/compilada/res/2021/resolucao-no-23-673-14-de-dezembro-de-2021>. Accessed: 2022-07-22.
- Kastelan, I., Kukulj, S., Pekovic, V., Marinkovic, V., and Marceta, Z. (2012). Extraction of text on tv screen using optical character recognition. In *2012 IEEE 10th Jubilee International Symposium on Intelligent Systems and Informatics*, pages 153–156. IEEE.
- Kwon, K.-S. and Ready, S. (2014). Practical guide to machine vision software: an introduction with labview. John Wiley & Sons.
- Mariappan, M., Ramu, V., Ganesan, T., Khoo, B., and Vellian, K. (2011). Virtual medical instrument for otorob based on labview for acquiring multiple medical instrument lcd reading using optical character recognition. In *2011 International Conference on Biomedical Engineering and Technology, IPCBEE vol, volume 11*.
- Mittal, A., Moorthy, A. K., and Bovik, A. C. (2012a). No-reference image quality assessment in the spatial domain. In *IEEE Transactions on Image Processing*, volume 21, pages 4695–4708. IEEE.
- Mittal, A., Soundararajan, R., and Bovik, A. C. (2012b). Making a “completely blind” image quality analyzer. In *IEEE Signal Processing Letters*, volume 20, pages 209–212. IEEE.
- Pech-Pacheco, J. L., Cristóbal, G., Chamorro-Martinez, J., and Fernández-Valdivia, J. (2000). Diatom autofocusing in brightfield microscopy: a comparative study. In *Proceedings 15th International Conference on Pattern Recognition. ICPR-2000*, volume 3, pages 314–317. IEEE.
- Qin, H. and El-Yacoubi, M. A. (2017). Deep representation for finger-vein image-quality assessment. In *IEEE Transactions on Circuits and Systems for Video Technology*, volume 28, pages 1677–1693. IEEE.
- Shrivakshan, G. and Chandrasekar, C. (2012). A comparison of various edge detection techniques used in image processing. In *International Journal of Computer Science Issues (IJCSI)*, volume 9. Citeseer.
- Smith, R. (2007). An overview of the tesseract ocr engine. In *Ninth international conference on document analysis and recognition (ICDAR 2007)*, volume 2, pages 629–633. IEEE.
- Tekin, E., Coughlan, J. M., and Shen, H. (2011). Real-time detection and reading of led/lcd displays for visually impaired persons. In *2011 IEEE Workshop on Applications of Computer Vision (WACV)*, pages 491–496. IEEE.